Large fluctuations and singular behavior of nonequilibrium systems

D. Pinna[*] and A. D. Kent[†]

Department of Physics, New York University, New York, New York 10003, USA

D. L. Stein[‡]

Department of Physics, New York University, New York, New York 10003, USA;
Courant Institute of Mathematical Sciences, New York University, New York, New York 10012, USA;
and NYU-ECNU Institutes of Physics and Mathematical Sciences at NYU Shanghai, 3663 Zhongshan Road North, Shanghai, 200062, China

We present a general geometrical approach to the problem of escape from a metastable state in the presence of noise. The accompanying analysis leads to a simple condition, based on the norm of the drift field, for determining whether caustic singularities alter the escape trajectories when detailed balance is absent. We apply our methods to systems lacking detailed balance, including a nanomagnet with a biaxial magnetic anisotropy and subject to a spin-transfer torque. The approach described within allows determination of the regions of experimental parameter space that admit caustics.

I. INTRODUCTION

A noisy dynamical system will occasionally experience large fluctuations that can dramatically alter its state. These fluctuations are responsible for a wide variety of interesting behaviors, including stochastic resonance [1,2], transport via Brownian ratchets [3,4], logarithmic susceptibility in driven nonadiabatic systems [5], and Brownian vortices [6,7]. In the limit of weak noise, the system's dynamical response is determined by its optimal paths, i.e., the paths along which it moves with maximum probability [8,9].

Because probability ρ is conserved in a closed system, it satisfies a continuity equation: $\partial \rho / \partial t + \boldsymbol{\nabla} \cdot \mathbf{J} = 0$, where J is the probability current determined by the Fokker-Planck equation that governs the time evolution of ρ. For a system in equilibrium, detailed balance is satisfied; in the present context, this corresponds to $J = 0$ at every point in space. When detailed balance holds, fluctuational trajectories behave in a simple fashion, to be discussed in Sec. III. However, when the system's stationary probability distribution lacks detailed balance, the fluctuational trajectories (also known as optimal paths) can exhibit unusual behavior. In particular, singularities known as *caustics* (defined in Sec. V) can develop in the action of the stationary (or quasistationary, depending on choice of boundary conditions) density [4,10–14]; these result from folds and cusps in the projection of the Lagrangian manifold of escape trajectories onto the original space of the dynamical variables [11]. Such singularities cannot occur in the presence of detailed balance, but in its absence their presence can significantly alter the behavior of noise-induced escape from a static metastable state [11,13] or a limit cycle [15,16]. Optimal trajectories avoid caustics [11], so appearance of a caustic in the vicinity of a stable or saddle point can dramatically alter the escape behavior [13].

In this paper, we reformulate the escape problem and in so doing determine conditions under which singularities in the optimal escape trajectories can appear. This leads to a new approach, based on a simple feature of the deterministic (i.e., zero-noise) dynamics, toward determining the presence and behavior of caustics. We apply our approach, first to a previously studied system [13] in which caustics are known to dramatically affect the escape dynamics, and then to a system not studied from this perspective, namely magnetic reversal in a biaxial nanomagnet subject to both thermal noise and spin-transfer torque. For the latter system we determine the experimental parameter ranges for which caustics are likely (and unlikely) to occur.

II. ESCAPE IN A NOISY DYNAMICAL SYSTEM

Consider an overdamped particle with position vector $\mathbf{x}(t)$ in an n-dimensional space. If the particle is subject to both deterministic and random forces, its time evolution in the general case is described by the Langevin equation

$$\dot{\mathbf{x}} = \mathbf{F}(\mathbf{x}) + \sqrt{2\epsilon}\hat{\mathbf{H}} \cdot \dot{\mathbf{W}}, \qquad (1)$$

where $\mathbf{F}(\mathbf{x})$ denotes the drift field, $\dot{\mathbf{W}}$ represents a white-noise process, and the tensor $\hat{\mathbf{H}}(\mathbf{x})$ and scalar ϵ characterize the noise anisotropy and strength, respectively. The term $\hat{\mathbf{H}}(\mathbf{x})$ is generally an $n \times d$ matrix, with n the dimensionality of the system's configuration space and d the dimensionality of the noise. If $\hat{\mathbf{H}}(\mathbf{x})$ has an explicit dependence on x, then the noise is multiplicative and should be understood in the Itô sense. We take ϵ to be sufficiently small so that the timescale of a successful escape is long compared to that of a single excursion from the stable point.

Diagonalizing Eq. (1), we let $\hat{\mathbf{G}}$ be the diagonal matrix with $\hat{G}_{ii} = g_i^2$ corresponding to $\hat{\mathbf{H}}$. The associated drift-field vector then has components $f_i = F_i / g_i^2$, which can be seen as follows. In terms of its components, the stochastic contribution on the right-hand side of Eq. (1) can be written in terms of a single Wiener process with compound variance:

$$\sum_j \hat{H}_{i,j}\, W_j = g_i\, \tilde{W}, \qquad (2)$$

---

[*]Current address: Unité Mixte de Physique CNRS/Thales, 1 Avenue Augustin Fresnel, 91767 Palaiseau, France; daniele.pinna@nyu.edu

[†]andy.kent@nyu.edu

[‡]daniel.stein@nyu.edu

where $g_i^2 = \sum_j \hat{H}_{i,j}^2$ and $\tilde{W}$ is identical to the original Wiener process, now driving each component of the original Langevin equation.

We can then rewrite Eq. (1) as

$$\dot{\mathbf{x}} = \mathbf{F}(\mathbf{x}) + \sqrt{2\epsilon}\mathbf{g}(\mathbf{x})\dot{\tilde{W}}, \qquad (3)$$

and for each of the n components of the Langevin equation, we can write

$$2\epsilon \dot{\hat{W}}^2 = \frac{1}{g_i^2}(\dot{x}_i - F_i)^2. \qquad (4)$$

The quasistationary distribution $\rho(\mathbf{x}) \propto \exp[-S(\mathbf{x})/2\epsilon]$ is given to leading order in the zero-noise limit [8] by the variational problem consisting of finding the extrema of the action functional $S = \int_0^T L_{\mathrm{FW}}\, dt$. That is, one varies over all paths beginning at a fixed reference point x_0 and ending at the point x of interest at time T, and chooses the one that minimizes the action. Summing over the components in Eq. (4), one arrives at the *Freidlin-Wentzell* (FW) Lagrangian and associated Hamiltonian in the action functional:

$$L_{\mathrm{FW}} = \tfrac{1}{2}(\dot{\mathbf{x}} - \mathbf{F}) \cdot \hat{G}^{-1} \cdot (\dot{\mathbf{x}} - \mathbf{F}), \qquad (5)$$

$$H_{\mathrm{FW}} = \tfrac{1}{2}[(\mathbf{p} + \mathbf{f}) \cdot \hat{G} \cdot (\mathbf{p} + \mathbf{f}) - \mathbf{f} \cdot \hat{G} \cdot \mathbf{f}]. \qquad (6)$$

Here $\mathbf{f} = \hat{G}^{-1} \cdot \mathbf{F}$ and $\mathbf{p}$ is the FW canonical momentum with elements $p_i = \partial_{\dot{x}_i} L_{\mathrm{FW}}$.

Suppose now that the drift field contains one or more stable fixed points and that the system's initial state lies within the basin of attraction of one of these. It can be seen by inspection of Eq. (6) that the fluctuational dynamics can be mapped onto the problem of a particle with unit electrical charge moving on a Riemannian manifold with (positive definite) metric tensor $\hat{\mathbf{G}}$, under the combined influence of a magnetic vector potential $\mathbf{A} = -\mathbf{f}$ [17] and electric scalar potential $\phi = -\mathbf{f} \cdot \hat{G} \cdot \mathbf{f} = -|\mathbf{f}|_{\hat{G}}^2$ [18]. Hamilton's equations of motion are then

$$\dot{\mathbf{x}} = \hat{G} \cdot \mathbf{p} + \mathbf{F} = \hat{G} \cdot (\mathbf{p} + \mathbf{f}), \qquad (7)$$

$$\dot{\mathbf{p}} = -\nabla_{\mathbf{x}} H_{\mathrm{FW}}. \qquad (8)$$

The optimal escape paths are zero-energy trajectories, that is, those along which the Hamiltonian Eq. (6) vanishes (see, for example, Ref. [19]). For any state vector $\mathbf{x}$, the set of momenta satisfying the zero-energy condition $H_{\mathrm{FW}} = 0$ can be seen to describe an n-dimensional ellipse in momentum space centered at $\mathbf{p} = -\mathbf{f}$ and with axes $a_i = \sqrt{\mathbf{f} \cdot \hat{G} \cdot \mathbf{f}/g_i^2}$.

III. THE MOMENTUM ELLIPSE

For simplicity we now confine our considerations to two dimensions; the procedure presented below is straightforwardly generalized to higher dimensions by parametrizing an n-dimensional ellipse. The 2D momentum ellipse can be parametrized as

$$p_x(\gamma) = \frac{|\mathbf{f}|_{\hat{G}}}{g_x} \cos\gamma - f_x, \qquad (9)$$

$$p_y(\gamma) = \frac{|\mathbf{f}|_{\hat{G}}}{g_y} \sin\gamma - f_y. \qquad (10)$$
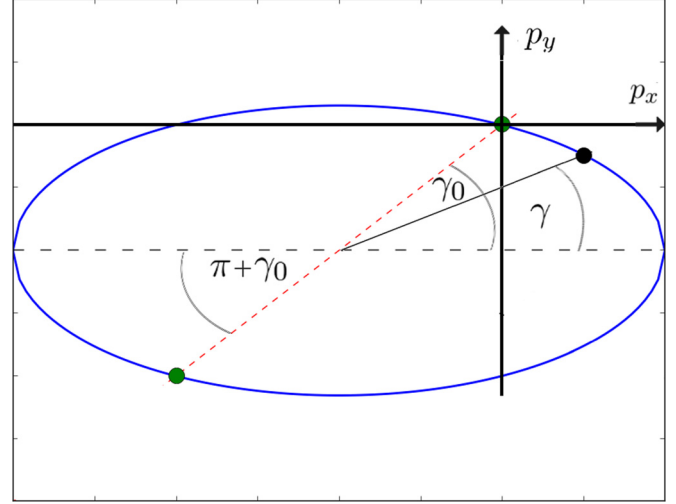

FIG. 1. Diagram of momentum ellipse parametrized by γ. γ_0 and $\pi + \gamma_0$ correspond to anti-instanton and instanton solutions, respectively.

This momentum ellipse defines all possible least-action motions accessible to the particle at $\mathbf{x}$ traveling along an escape trajectory. The so-called "anti-instanton" trajectories characterize motion toward the stable fixed point; these have zero FW momentum and travel parallel to the drift field, corresponding to $\gamma = \gamma_0 \equiv -\arctan(\frac{f_y}{f_x}\frac{g_y}{g_x})$. The so-called "instanton" trajectories, i.e., fluctuational paths away from the stable fixed point, travel antiparallel to the drift field in systems with detailed balance (see below) and have a corresponding FW momentum $\bar{p} = -2\bar{f}$ [8,19,20], which here corresponds to $\gamma = \pi + \gamma_0$. Figure 1 shows a typical diagram of such a momentum ellipse.

Because the angle γ parametrizes momentum at each point in configuration space, it is convenient to express the equations of motion of the particle trajectories solely as a function of $\mathbf{x}$ and γ. Substituting Eqs. (9) and (10) into the Hamiltonian equations of motion, Eqs. (7) and (8), we find

$$\dot{x} = g_x |\mathbf{f}|_{\hat{G}} \cos\gamma, \\ \dot{y} = g_y |\mathbf{f}|_{\hat{G}} \sin\gamma. \qquad (11)$$

The role of γ in characterizing the direction of escape is apparent. The slope of the escape trajectory is found by dividing the second of Eq. (11) by the first to yield

$$\partial y/\partial x = (g_y/g_x) \tan\gamma. \qquad (12)$$

IV. THE NATURE OF FLUCTUATIONAL TRAJECTORIES

Equations (11) show that thermally driven dynamics evolve at the rate of the deterministic dynamics rescaled by the noise-induced metric, i.e., $|\dot{x}|_{\hat{G}^{-1}}^2 = |\mathbf{f}|_{\hat{G}}^2 = |\mathbf{F}|_{\hat{G}^{-1}}^2$. When the noise is additive ($\hat{\mathbf{H}}$ independent of x) and isotropic ($\hat{\mathbf{G}} \equiv \hat{\mathbf{1}}$) [21], detailed balance is satisfied if the drift field is derivable as the gradient of a smooth potential function [13,19]. In this case the two rates become trivially identical, because the instanton ($\dot{\mathbf{x}} = -\mathbf{f}$) and anti-instanton ($\dot{\mathbf{x}} = \mathbf{f}$) trajectories are simply sign-reversed. It is somewhat surprising, however, to see that it holds more generally. This result can alternatively be derived

by writing down the effective Lorentz dynamics for a charged particle traveling in both electric and magnetic fields,

$$\ddot{\mathbf{x}} = \nabla|\mathbf{f}|^2 - \dot{\mathbf{x}} \times (\nabla \times \mathbf{f}), \tag{13}$$

and noting that upon multiplying by $\dot{\mathbf{x}}$ one obtains $\partial_t|\dot{\mathbf{x}}|^2 = \partial_t|\mathbf{f}|^2$, again implying that the dynamical speed of a particle moving under the influence of noise is equal to the norm of the zero-noise drift field. This notion has been employed in the literature [22] to construct an efficient numerical scheme (the *gMAM* method, which represents an evolution of the minimum action method [23]) capable of computing transition pathways via geometric minimization of the FW action, improving on the older String method [24,25].

Using these results, the Freidlin-Wentzel Lagrangian can be rewritten as [26]

$$\begin{aligned} L_{\text{FW}} &= \tfrac{1}{2}|\dot{\mathbf{x}} - \mathbf{F}|^2_{\hat{\mathbf{G}}^{-1}} = \tfrac{1}{2}\big[|\dot{\mathbf{x}}|^2_{\hat{\mathbf{G}}^{-1}} + |\mathbf{F}|^2_{\hat{\mathbf{G}}^{-1}} - 2\dot{\mathbf{x}} \cdot \hat{\mathbf{G}}^{-1} \cdot \mathbf{F}\big] \\ &= |\mathbf{f}|^2_{\hat{\mathbf{G}}} - \dot{\mathbf{x}} \cdot \mathbf{f} \\ &= |\mathbf{f}|^2_{\hat{\mathbf{G}}}(1 - \cos\Psi), \end{aligned} \tag{14}$$

where we have employed the identities $\mathbf{F} = \hat{\mathbf{G}} \cdot \mathbf{f}$ and $\dot{\mathbf{x}} \cdot \hat{\mathbf{G}}^{-1} \cdot \dot{\mathbf{x}} = |\mathbf{f}|^2_{\hat{\mathbf{G}}}$, and defined

$$\Psi \equiv \arccos\left(\frac{\dot{\mathbf{x}} \cdot \mathbf{f}}{|\mathbf{f}|^2_{\hat{\mathbf{G}}}}\right) \tag{15}$$

as the angle between the instantaneous escape velocity $\dot{\mathbf{x}}$ and the deterministic drift field $\mathbf{f}$ at $\mathbf{x}$. Equation (14), which is exact in the low-noise limit, shows that, as long as Ψ does not vary too much over the course of the escape trajectory, the effective action $S(\mathbf{x})$ will be dominated by the behavior of $|\mathbf{f}|_{\hat{\mathbf{G}}}$, implying that the norm of the drift field alone captures much of the structure of the system's action.

To characterize better the relative importance of $|\mathbf{f}|$ versus Ψ on the escape dynamics, consider a closed fluctuational path $\mathcal{C}$ that moves from a stable fixed point $\mathbf{x_S}$ to some other point $\mathbf{x_0}$ within its attractive basin, subsequently returning (along the anti-instanton trajectory $\dot{\mathbf{x}} = \mathbf{f}$) to the fixed point. Using $\Omega_\mathcal{C}$ to denote the surface enclosed by $\mathcal{C}$, we find

$$S_\mathcal{C} = \oint_\mathcal{C} \big(|\mathbf{f}|^2_{\hat{\mathbf{G}}} - \dot{\mathbf{x}} \cdot \mathbf{f}\big)dt = \oint_\mathcal{C} ds|\mathbf{f}|_{\hat{\mathbf{G}}} - \int d\Omega_\mathcal{C} \cdot (\nabla \times \mathbf{f}). \tag{16}$$

In the second equality we changed integration variables from t to s, where s denotes distance traveled along the trajectory, and used the earlier result that $|\dot{\mathbf{x}}| = |\mathbf{f}|$ for all systems. We also used Stokes' theorem to rewrite the effect of the geometrical phase due to Ψ in terms of its equivalent surface integral. This equation shows how the presence of a nongradient field (which possesses nonzero curl) contributes to the action, and therefore helps determine the trajectory, of an optimal path. While enclosing a larger "magnetic flux" $\int d\Omega_\mathcal{C} \cdot (\nabla \times \mathbf{f})$ acts to reduce the path's action (where the flux term is positive), doing so can also move the particle into regions of configuration space with larger $|\mathbf{f}|$, which acts to increase the action. The least action trajectory therefore optimizes the relative balance between these two terms.

There are two immediate consequences of Eq. (16). The first is that in gradient systems, where $\mathbf{f} = -\nabla_\mathbf{x}U$ for some

smooth potential function $U(\mathbf{x})$ (so $\nabla \times \mathbf{f} = 0$), and where the instanton trajectory satisfies $\dot{\mathbf{x}} = -\mathbf{f}$, we recover the well-known action (see, for example, Ref. [19]) for the entire trajectory: $S_\mathcal{C} = 2[U(\mathbf{x_0}) - U(\mathbf{x_S})]$. The second, more general consequence is that any sudden change in $|\mathbf{f}|$, as system parameters are varied, can dramatically alter the balance between the drift norm and the magnetic flux, and hence the structure of the optimal paths.

V. APPLICATIONS

When detailed balance is satisfied, fluctuational trajectories—i.e., instantons and anti-instantons—follow the drift field, and therefore never cross. When detailed balance is broken, anti-instantons still run parallel to the drift field [19], but now instantons need not run antiparallel; as a consequence, fluctuational trajectories can cross. Because the action is determined from the fluctuational trajectories (Sec. II), it will now in general be nondifferentiable at such crossing points. The envelope of crossing trajectories constitutes a caustic [27] (see, e.g., Fig. 1 of [14]). When caustics appear along the optimal escape trajectory, they can significantly alter the system's escape dynamics. In this section we consider two applications of the approach described in this paper: the first is to a well-studied system in which new insights are gained by utilizing this approach, and the second is to a system of physical interest that has not been previously studied from this perspective.

A. System with a tunable parameter

It has been observed [11,13] that noisy systems with nongradient deterministic dynamics (and therefore generally lacking detailed balance) containing tunable parameters can dramatically change their escape behaviors, in a way reminiscent of a broken symmetry transition, when certain critical parameter thresholds are crossed. Consider, for example, the following well-studied system [13] with a tunable parameter α:

$$\dot{x} = x(1 - x^2 - \alpha y^2) + \sqrt{\epsilon}\dot{W}_x, \tag{17}$$

$$\dot{y} = -y(1 + x^2) + \sqrt{\epsilon}\dot{W}_y, \tag{18}$$

where the additive white noise is isotropic and the drift field is nongradient for all $\alpha \neq 1$. For any α, the system has two stable fixed points at $(\pm 1, 0)$ and one hyperbolic (saddle) fixed point at $(0,0)$. We consider the optimal escape trajectory from $(1,0)$ to $(0,0)$, which flows along the x axis for $\alpha < 4$. Above $\alpha = 4$, however, caustics appear in the basin of attraction of the stable point [13], focusing to a point on the x axis between 0 and 1, as shown in Fig. 2. As a consequence, the optimal escape trajectory bifurcates into two off-axis trajectories. Analysis of the norm of the drift field reveals that in transitioning across the critical threshold $\alpha_C = 4$, the structure of the extrema of $\mathbf{f}$ changes abruptly. For $\alpha < 4$, the norm exhibits two global minima at $(1,0)$ and $(0,0)$, along with a saddle near the midpoint of the x axis. For $\alpha > 4$, however, two local minima appear symmetrically displaced off the x axis, with the previous on-axis saddle now a local maximum (Fig. 2). According to Eq. (14), these new minima lower the effective
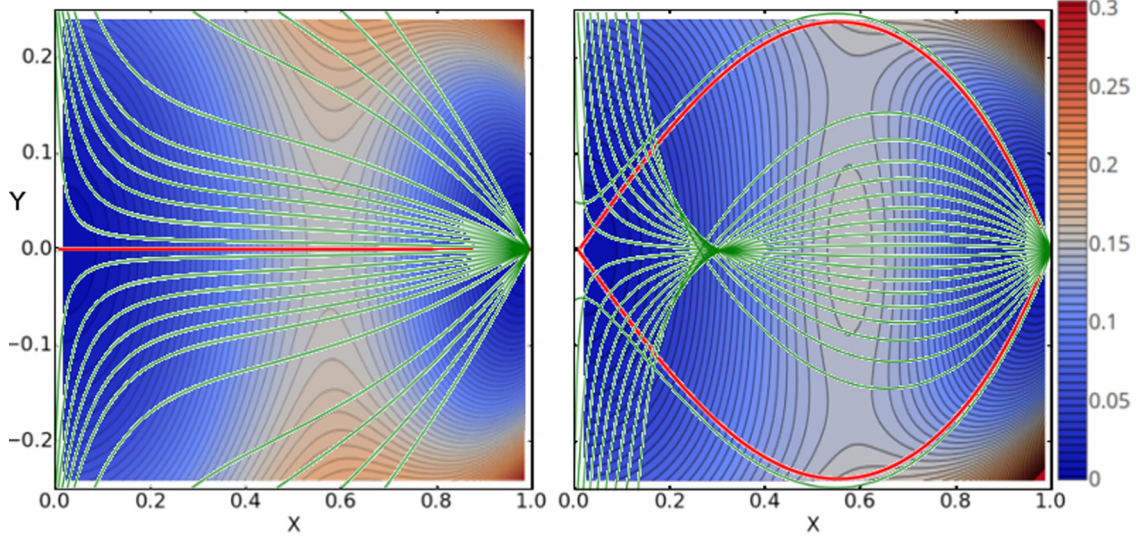
FIG. 2. Contour plot of the norm of the drift field from Ref. [13], for $\alpha = 3$ (left) and $\alpha = 5$ (right). Optimal escape trajectories are shown in red (medium gray), and other instanton trajectories in green (light gray). For $\alpha = 3$, instanton trajectories do not cross, and the escape trajectory lies along the x axis. Correspondingly, two global minima in the norm of the drift field are present at the unstable (0,0) and stable (1,0) equilibria, respectively, along with a saddle close to the midpoint of the x axis. For $\alpha = 5$, instanton trajectories cross, indicating the presence of a caustic (not shown). Correspondingly, the saddle in the norm of the drift field for $\alpha = 3$ is now a local maximum, with two new local minima appearing off the x axis. Consequently, there are now two symmetrical off-axis optimal escape trajectories that follow the new off-axis minima in the norm of the drift field (and in so doing avoid the caustic). A standard "shooting method" was employed to compute the trajectories. The FW dynamical equations were solved directly by evolving initial states taken very close to the fixed point of the drift field. Initial momenta were chosen to satisfy a gradient-like solution $\mathbf{p}(\mathbf{x}) = -2\mathbf{F}(\mathbf{x})$. The accuracy of this approach is guaranteed by the fact that in the neighborhood of a fixed point, the deterministic drift can always be approximated by the gradient of a potential.

action of off-axis escape trajectories, in accordance with observations. Deviation of the escape trajectories from the exact minima are due to the "magnetic flux" term in Eq. (16).

B. Biaxial macrospin subject to thermal noise and spin torque

A more interesting application is to a physically relevant model lacking detailed balance: the stochastic Landau-Lifshitz-Gilbert-Slonczewski (sLLGS) equation governing the evolution of a unit magnetization vector subject to a combination of both gradient and nongradient torques. This equation reads

$$\dot{m}_i = A_i(\mathbf{m}) + B_{ik}(\mathbf{m}) \circ H_{\text{th},k}, \qquad (19)$$

where the drift vector $\mathbf{A}(\mathbf{m})$ and diffusion matrix $\hat{\mathbf{B}}(\mathbf{m})$ are given by

$$\mathbf{A}(\mathbf{m}) = \mathbf{m} \times \mathbf{h}_{\text{eff}} - \alpha \mathbf{m} \times (\mathbf{m} \times \mathbf{h}_{\text{eff}})$$
$$- \alpha I \mathbf{m} \times (\mathbf{m} \times \hat{\mathbf{n}}_p), \qquad (20)$$

$$B_{ik}(\mathbf{m}) = \sqrt{C}[-\epsilon_{ijk}m_j - \alpha(m_i m_k - \delta_{ik})], \qquad (21)$$

and the equation is interpreted in the Stratonovich sense [28]. The first term in $\mathbf{A}(\mathbf{m})$ corresponds to magnetization precession about a local magnetic field, with $\mathbf{h}_{\text{eff}} = -\nabla_{\mathbf{m}} \epsilon(\mathbf{m})$ a conservative vector field. Here $\epsilon(\mathbf{m})$ is the energy landscape of the magnetic system under study. The second term in $\mathbf{A}(\mathbf{m})$ is a phenomenological damping term, with the damping constant α typically $\sim O(10^{-2})$. The third is a nongradient term corresponding to spin-angular momentum per unit time injected via a current I into the macrospin along an arbitrary

polarization direction $\hat{\mathbf{n}}_p$ [29]. Although the diffusion matrix $\hat{\mathbf{B}}(\mathbf{m})$ (with C the diffusion constant) appears state-dependent, it can be shown (e.g., by rewriting the dynamics in spherical coordinates) to correspond to isotropic, state-independent noise.

In the absence of applied currents ($I = 0$), the fluctuational trajectories are determined by the energy landscape $\epsilon(\mathbf{m})$ and do not cross. In the presence of nonvanishing current, however, detailed balance is absent, and it therefore becomes important to determine how this new feature may—or may not—alter the escape dynamics. The methods developed above allow us to analyze this problem by examining the norm of the total drift field governing the macrospin dynamics. To lowest order in α, it is

$$|\mathbf{A}(\mathbf{m})|^2 = |\mathbf{m} \times \mathbf{h}_{\text{eff}}|^2 + 2\alpha I \hat{\mathbf{n}}_p \cdot (\mathbf{m} \times \mathbf{h}_{\text{eff}}) + O(\alpha^2). \quad (22)$$

We wish to determine under which conditions the conservative precessional contribution dominates the nongradient contribution. That is, under which conditions do the extrema of $|\mathbf{A}(\mathbf{m})|^2$ corresponding to $I = 0$ not change significantly when $I > 0$? By the approach developed above, this implies that under such conditions the most probable escape paths should not differ significantly from the reverse-drift instanton paths of the purely gradient case.

We consider for simplicity the case of a biaxial macrospin subject to the energy landscape

$$\epsilon(\mathbf{m}) = D m_x^2 - m_z^2, \qquad (23)$$

defined on the surface of the unit sphere ($|\mathbf{m}| = 1$). Here $D \geqslant 0$ is the ratio of hard-axis to easy-axis anisotropies [30,31].
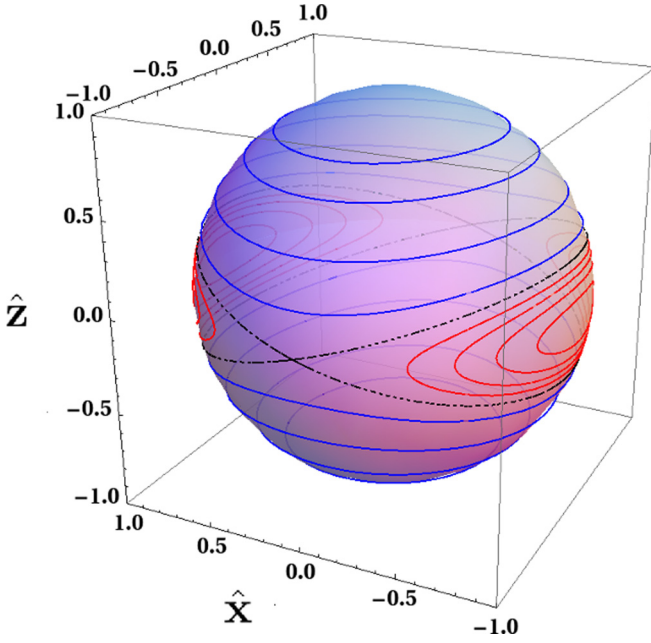
FIG. 3. Constant energy contours of the unit magnetization sphere. Red (medium gray) and blue (dark gray) contours correspond to $\epsilon < 0$ and $\epsilon > 0$ precessions, respectively. Dashed black lines are the $\epsilon = 0$ separatrices.

In the absence of applied currents and damping, the motion is purely precessional. Focusing solely on this precessional motion, we can divide the unit magnetization sphere into four disjoint dynamical regions, as shown in Fig. 3.

When magnetization energy is conserved, the surface of the sphere can be divided into trajectories with $\epsilon > 0$ and those with $\epsilon < 0$. The $\epsilon < 0$ surface can be further subdivided into orbits with $m_z > 0$ and $m_z < 0$, and the $\epsilon > 0$ surface similarly subdivided into orbits with $m_x > 0$ and $m_x < 0$. These regions are separated by a common separatrix $m_x = \pm m_z/\sqrt{D}$, corresponding to a degenerate $\epsilon = 0$ dynamical state whose trajectory lies on a plane tilted at an angle $\theta_C = \arctan(1/\sqrt{D})$ with respect to the $y-z$ plane.

However, the above description must be modified when damping and current are taken into account, since either will cause the magnetization energy $\epsilon(\mathbf{m})$ to change over time. Using Eqs. (19)–(21) and the definition $\mathbf{h}_{\text{eff}} = -\nabla_{\mathbf{m}}\epsilon(\mathbf{m})$, we find

$$\dot{\epsilon} = \nabla_{\mathbf{m}}\epsilon \cdot \dot{\mathbf{m}} = -\alpha[\mathbf{m} \times (\mathbf{h}_{\text{eff}} + I\hat{\mathbf{n}}_p)] \cdot (\mathbf{m} \times \mathbf{h}_{\text{eff}}). \quad (24)$$

Several qualitative conclusions can be drawn from Eq. (24). When $I = 0$, dissipation relaxes the system to one of the two negative energy basins in an effort to align the magnetization with the z axis. The addition of current (which we will conventionally choose to be negative, $I < 0$) leads to a progressive destabilization of the $m_z > 0$ negative-energy basin in favor of that at $m_z < 0$. More generally, the presence of current alters the boundaries of the attractive stable basins, even though a proper energy function that includes the spin-torque terms cannot be written. However, one can show that there exists a critical value $D_0 \approx 5.09$ that separates two distinctly different qualitative regimes [30]. In the $D < D_0$ case, the current alters the $\epsilon = 0$ separatrix boundary, while in the $D > D_0$ case, the

$\epsilon = 0$ boundary remains intact while the stable fixed points are modified by the current's action. Furthermore, above a critical current I_C (to be discussed further below) the entire $m_z > 0$ region becomes unstable, thereby eliminating the bistability of the magnetic system.

We want to determine under which conditions the nongradient current term can alter the fixed-point structure of the norm of the drift field. Because of the smallness of α, energy changes slowly, so one can still gain useful information by studying the norm of the drift along a constant negative-energy trajectory. Along each energy level set ϵ, one can compute the maxima and minima of the two terms appearing on the right-hand side of Eq. (19). This allows us to determine the range of experimental parameters for which the precessional term dominates, and therefore when effects due to nongradient terms can safely be ignored. Using Eq. (22) and the definition of $\mathbf{h}_{\text{eff}}$, we find the minimum of the precessional term along a particular constant energy contour to be

$$\min\{|\mathbf{m} \times \mathbf{h}_{\text{eff}}|^2\} = 4\min\{\epsilon(D - \epsilon) + (D + 1)m_z^2\}$$
$$= 4|\epsilon|(1 - |\epsilon|), \quad (25)$$

where we used the fact that $\min\{m_z^2\} = -\epsilon$ along a constant negative-energy contour.

We next consider the maximum of the nongradient current term in Eq. (19) and, for definiteness, we limit ourselves to cases where $\hat{\mathbf{n}}_p$ lies in the $x-z$ plane. Let ω denote the fixed tilt angle that $\hat{\mathbf{n}}_p$ makes with the z axis, and I_C denote the critical applied current above which the entire $m_z > 0$ region becomes unstable. Then for small α, $I_C = (2/\pi)\sqrt{D(D + 1)}/\cos\omega$ when $D > D_0$ and $I_C = (D + 2)/2\cos\omega$ when $D < D_0$ [30]. Using these results, we find

$$\max\{2\alpha I\hat{\mathbf{n}}_p \cdot (\mathbf{m} \times \mathbf{h}_{\text{eff}})\}$$
$$= (4\alpha I_C \cos\omega)\max\{m_y(Dm_x + m_z\tan\omega)\}$$
$$= \begin{cases} 4\alpha\sqrt{|\epsilon|(1 - |\epsilon|)}\tan\omega, & \text{if } D = 0 \\ \frac{8\alpha}{\pi}\sqrt{D(D + 1)(D + |\epsilon|)|\epsilon|}\, Q(\omega), & \text{if } D > D_0, \quad (26) \\ 2\alpha(D + 2)\sqrt{(D + |\epsilon|)|\epsilon|}\, Q(\omega), & \text{if } D < D_0 \end{cases}$$

where

$$Q(\omega)$$
$$= \max_{m_z}\left\{\sqrt{1 - \frac{(D + 1)m_z^2}{D + |\epsilon|}}\left[\sqrt{\frac{m_z^2}{|\epsilon|} - 1} + \frac{\tan\omega}{\sqrt{D}}\frac{m_z}{\sqrt{|\epsilon|}}\right]\right\}, \quad (27)$$

and we set the current I equal to I_C in each case to obtain an upper bound.

The above equations reveal a quantitative difference between the small tilt ($\tan\omega \ll \alpha^{-1}$) and large tilt ($\tan\omega \gg \alpha^{-1}$) cases. Consider first the case $D = 0$. By Eqs. (25) and (26), the precessional term dominates the nongradient term when $\epsilon(1 - \epsilon) \gg \alpha^2\tan^2\omega$. For the small tilt case, as long as the magnetization energy is not too close to the separatrix ($\epsilon = 0$) or the $m_z = 1$ pole ($|\epsilon| = 1$), the precessional term dominates and no caustics will be present. More precisely, the precessional term dominates within the energy range $\alpha^2\tan^2\omega < |\epsilon| < 1 - \alpha^2\tan^2\omega$. When the tilt is larger, on the other hand, the nongradient term begins to compete, and the

presence of caustics *may* affect the reversal dynamics. Whether they do requires a detailed analysis of the particular case of interest.

This conclusion remains qualitatively unchanged when $D > D_0$, with the main quantitative change being that the energy range in which caustics cannot appear in the small tilt case is now $D\alpha \tan \omega < |\epsilon| < 1 - D\alpha \tan \omega$. For $D < D_0$, we need to further subdivide into the $D > |\epsilon|$ and $D < |\epsilon|$ cases. The latter smoothly goes to the $D = 0$ case as D decreases, while the former gives the same result as the $D > D_0$ case.

Summarizing, we find that the presence of caustics is determined by the fixed tilt angle ω that $\hat{\mathbf{n}}_p$ makes with the z axis. For any D, the escape dynamics are unaffected by caustics for a wide energy range in the small tilt case ($\tan \omega \ll \alpha^{-1}$), but in principle the large tilt case ($\tan \omega \gg \alpha^{-1}$) can show substantially different behavior.

C. Analytical solution of the $\omega = 0$ case

In this section we analytically solve for the Hamiltonian dynamics arising from the FW action for the case of $\omega = 0$, with arbitrary applied current. In this case, the dynamics become effectively one-dimensional and the dynamical equations can be exactly solved. The FW Lagrangian for the thermally activated dynamics of the macrospin, expressed in spherical coordinates (θ, ϕ), is

$$L_{FW} = \tfrac{1}{2}[(\dot{\theta} - f_\theta)^2 + \sin^2(\theta)(\dot{\phi} - f_\phi)^2]. \quad (28)$$

Passing to the Hamiltonian formalism we have

$$H_{FW} = \frac{1}{2}\left[p_\theta^2 + \frac{p_\phi^2}{\sin^2(\theta)}\right] + p_\theta f_\theta + p_\phi f_\phi, \quad (29)$$

where p_θ and p_ϕ are the conjugate momenta of θ and ϕ.

Hamilton's equations are then

$$\dot{\theta} = p_\theta + f_\theta, \quad (30)$$

$$\dot{\phi} = \frac{p_\phi}{\sin^2 \theta} + f_\phi, \quad (31)$$

$$\dot{p}_\theta = \frac{\cos \theta}{\sin^3 \theta} p_\phi^2 - p_\theta \partial_\theta f_\theta - p_\phi \partial_\theta f_\phi, \quad (32)$$

$$\dot{p}_\phi = -p_\theta \partial_\phi f_\theta - p_\phi \partial_\phi f_\phi, \quad (33)$$

where so far all results are completely general and extensible to models of any complexity (anisotropy ratio $D \neq 0$, positive tilts between axes, etc.). For a macrospin with both $D = 0$ and $\omega = 0$, the drift vector field of the dynamics (expressed in terms of θ and ϕ) can be obtained by rewriting Eqs. (19)–(21) in spherical coordinates. Doing so, one finds

$$f_\theta = -\alpha(I + \cos \theta) \sin \theta, \quad (34)$$

$$f_\phi = -\cos \theta. \quad (35)$$

Because ϕ is a cyclic Hamiltonian variable, $p_\phi = c$ with c constant. For a zero-energy trajectory of Eq. (29), p_θ is given by

$$p_\theta = -f_\theta\left[1 \pm \sqrt{1 - c\left(2\frac{f_\phi}{f_\theta} + \frac{\alpha c}{\xi f_\theta \sin^2 \theta}\right)}\right]. \quad (36)$$
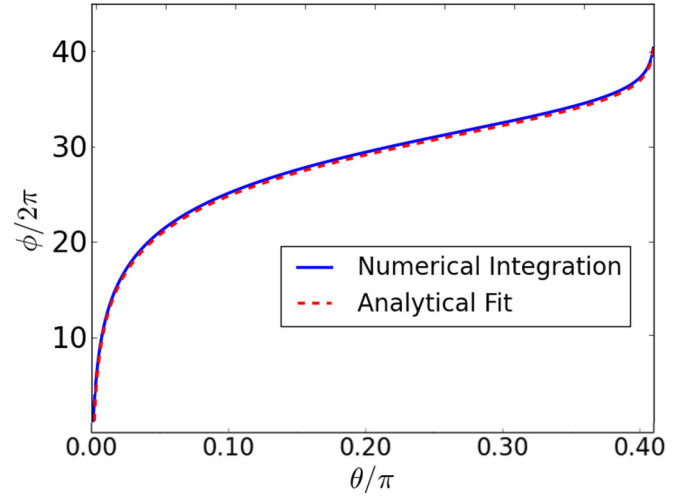

FIG. 4. Escape trajectory for a macrospin model with $\alpha = 0.01$, $D = 0$, $I = 0.3 I_C$, and $\omega = 0$. Blue (solid) line shows the least-action result of numerical integration of the FW dynamics. Red (dashed) line is the analytical result Eq. (14).

This solution is physically valid as long as the radicand is greater than or equal to zero for all values of θ in the range of interest. This implies that $c = 0$. The conjugate coordinate ϕ of p_ϕ then evolves along the deterministic drift field during the escape process, i.e., $\dot{\phi} = f_\phi$, and therefore $p_\theta = -f_\theta[1 \pm 1]$. The $p_\theta = 0$ solution corresponds as usual to relaxation to equilibrium, and the $p_\theta = -2 f_\theta$ solution corresponds to instanton escape, antiparallel to the drift, along the θ coordinate. However, during this process the precessional dynamics of ϕ remain unaltered, so escape from the stable well does not merely correspond to time-reversal of the deterministic dynamics.

Having solved for the general momenta in terms of the spherical coordinates, we can analytically derive the relation
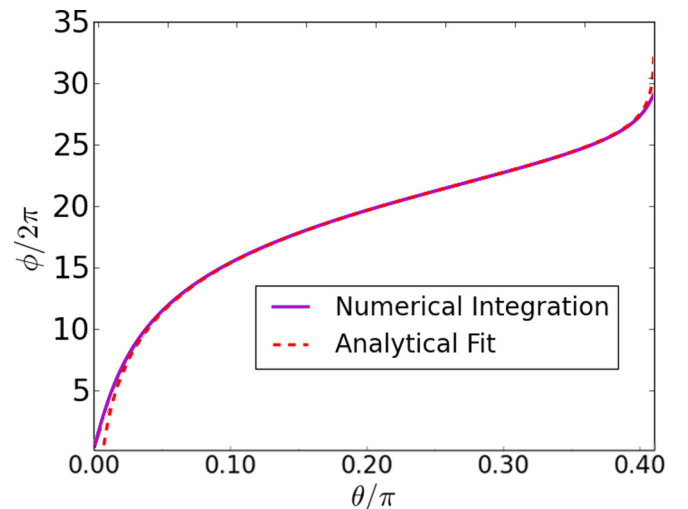

FIG. 5. Escape trajectory for a macrospin model with $\alpha = 0.01$, $D = 0$, $I = 0.3 I_C$, and $\omega = 0.3 \theta_C$ (defined in text). The purple (solid) line shows the least-action result of numerical integration of the FW dynamics. The red (dashed) line is the analytical result Eq. (14).
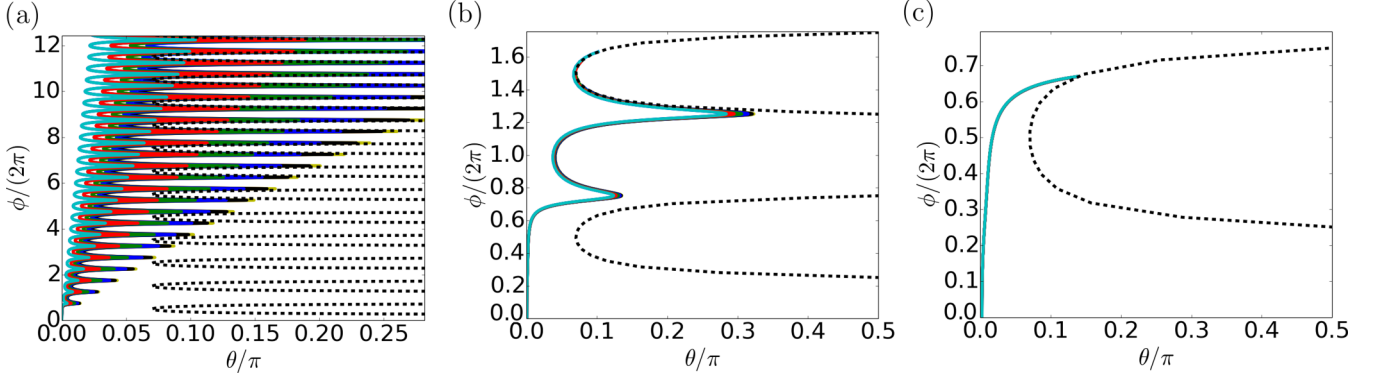
FIG. 6. Escape trajectory for macrospin model with $\alpha = 0.01$, $D = 20$, $I = 0.8\,I_C$, and varying tilts: (a) $\omega = 0$, (b) $\omega = 0.1\,\theta_C$, (c) $\omega = 0.25\,\theta_C$. Different color trajectories correspond to different initial conditions of the FW dynamics. Dashed black lines correspond to the $\epsilon = 0$ separatrices. In all scenarios, escape trajectories never cross, indicating the absence of caustics.

between ϕ and θ along the escape trajectories. Dividing $\dot{\phi}$ by $\dot{\theta}$ from Hamilton's equations, we find

$$
\begin{aligned}
\phi(\theta) &= \frac{1}{\alpha} \int_0^\theta d\tilde{\theta}\, \frac{\cos\tilde{\theta}}{(I + \cos\tilde{\theta})\sin\tilde{\theta}} \\
&= \frac{1}{\alpha(1 - I^2)}\left\{\log\left[\tan(\theta/2)\right] + I\log\left[\frac{2(I + \cos\theta)}{\sin\theta}\right]\right\},
\end{aligned}
\tag{37}
$$

where the integrand diverges at the $\theta = 0$ pole due to degeneracy in the ϕ coordinate, and at the $\theta = \arccos(-I)$ separatrix where the escape trajectory is nondifferentiable.

We tested these results and predictions by numerically integrating the FW dynamics associated with the stochastic process Eq. (16) for several different cases. The case $D \neq 0$ will be discussed in the following section. Here we show results for $D = 0$, with both zero and small tilt.

Figure 4 shows the optimal escape trajectory for $D = 0$, $\omega = 0$, and $I = 0.3\,I_C$. As shown above, the FW dynamics are exactly solvable in this case.

We next consider the case of small tilt. In accord with our analysis, the numerical results demonstrate that the escape dynamics are essentially unaltered (Fig. 5). In the limit of sufficiently small α, critical currents scale trivially with the tilt ($I_C^\omega = I_C^0 / \cos\omega$) [30]. By including this correction to the $\omega = 0$ escape model, we can fit the data well, even though the system no longer obeys detailed balance.

VI. DISCUSSION

We tested the predictions of the previous section by numerically integrating the FW dynamics associated with the stochastic process Eq. (19) for several different cases. Results for $D = 0$ were shown in Fig. 5. The absence of caustics, for both zero and small tilt, is apparent. Here we present the more interesting case of nonvanishing D. Figure 6 shows results for $D = 20$, $I = 0.8\,I_C$, and three tilts $\omega = 0, 0.1$, and $0.25\,\theta_C$ [recall that $\theta_C = \arctan(1/\sqrt{D})$]. These tilt values (and even larger ones) can be realized in current experiments on orthogonal spin-valve devices [32].

The optimal trajectories change as tilt is increased, even though the exit point remains essentially unchanged. However, numerical results for larger tilts, up to the critical tilt, do not exhibit crossing of escape trajectories, suggesting that caustics have not formed near escape paths. The only major difference is the number of precessions the system undergoes before reaching the separatrix (i.e., the boundary of the domain of attraction of the stable fixed point, which here corresponds to $\epsilon = 0$).

To summarize, an analysis of the norm of the drift field indicates that for most tilts, caustics do not appear within the escape region, and so—perhaps surprisingly—the loss of detailed balance does not qualitatively alter the escape dynamics. However, on closer examination one finds that for any tilt, there remain regions—where $m_z \approx 1$ or, separately, where $\epsilon \approx 0$—where this conclusion breaks down, because the precessional contribution to the drift norm vanishes at $m_z = 1$ and at $\epsilon = 0$. That is, two regions will always exist in the magnet's configuration space where the (nongradient) spin-transfer torque term dominates the (gradient) precessional term. The widths of these regions have been shown to be sufficiently small that their effect on the escape dynamics is negligible.

In the case when the tilt is large ($\tan\omega \gg \alpha^{-1}$), however, the nongradient term dominates the gradient term in all of configuration space, and so caustics *may* appear. In order to determine whether they do requires a more lengthy analysis, in which the fixed point structure of the drift field norm must be analyzed to determine whether it changes. We defer such an analysis to future work.

[1] L. Gammaitoni, P. Hänggi, P. Jung, and F. Marchesoni, Rev. Mod. Phys. **70**, 223 (1998).

[2] R. Löfstedt and S. N. Coppersmith, Phys. Rev. Lett. **72**, 1947 (1994).

[3] M. O. Magnasco, Phys. Rev. Lett. **71**, 1477 (1993).

[4] M. Millonas and M. I. Dykman, Phys. Lett. A **185**, 65 (1994).

[5] V. N. Smelyanskiy, M. I. Dykman, H. Rabitz, and B. E. Vugmeister, Phys. Rev. Lett **79**, 3113 (1997).

[6] B. Sun, J. Lin, E. Darby, A. Y. Grosberg, and D. G. Grier, Phys. Rev. E **80**, 010401(R) (2009).

[7] B. Sun, D. G. Grier, and A. Y. Grosberg, Phys. Rev. E **82**, 021123 (2010).

[8] M. I. Freidlin and A. D. Wentzell, *Random Perturbations of Dynamical Systems* (Springer, New York, 1984).

[9] M. I. Dykman and K. Lindenberg, in *Contemporary Problems in Statistical Physics*, edited by G. Weiss (SIAM, Philadelphia, 1994), p. 41.

[10] R. Graham and T. Tél, Phys. Rev. A **33**, 1322 (1986).

[11] M. I. Dykman, M. Millonas, and V. N. Smelyanskiy, Phys. Lett. A **195**, 53 (1994).

[12] R. S. Maier and D. L. Stein, Phys. Rev. Lett. **69**, 3691 (1992).

[13] R. S. Maier and D. L. Stein, Phys. Rev. Lett. **71**, 1783 (1993).

[14] O. Kogan, arXiv:1110.2820 (2011).

[15] V. N. Smelyanskiy, M. I. Dykman, and R. S. Maier, Phys. Rev. E **55**, 2369 (1997).

[16] R. S. Maier and D. L. Stein, Phys. Rev. Lett. **77**, 4860 (1996).

[17] M. I. Dykman and M. A. Krivoglaz, in *Synergetics and Cooperative Phenomena in Solids and Macromolecules* (Valgus, Tallin, 1983), pp. 33–44.

[18] Given a Riemannian metric $\hat{\mathbf{Q}}$, we will denote the inner product of two vectors **a** and **b** as $\langle \mathbf{a},\mathbf{b}\rangle_{\hat{\mathbf{Q}}}$. Analogously, the inner product on $\hat{\mathbf{Q}}$ of a vector with itself will be written $\langle \mathbf{a},\mathbf{a}\rangle_{\hat{\mathbf{Q}}} \equiv |\mathbf{a}|^2_{\hat{\mathbf{Q}}}$.

[19] R. S. Maier and D. L. Stein, Phys. Rev. E **48**, 931 (1993).

[20] M. Marder, Phys. Rev. Lett. **74**, 4547 (1995).

[21] Under these conditions the Riemannian manifold acquires a Euclidean metric.

[22] M. Heymann and E. Vanden-Eijnden, Phys. Rev. Lett. **100**, 140601 (2008).

[23] Weinan E, W. Ren, and E. Vanden-Eijnden, Comm. Pure Appl. Math. **57**, 637 (2004).

[24] Weinan E, W. Ren, and E. Vanden-Eijnden, Phys. Rev. B **66**, 052301 (2002).

[25] E. Weinan, W. Ren, and E. Vanden-Eijnden, J. Chem. Phys **126**, 164103 (2007).

[26] A similar reformulation appears in M. Heymann and E. Vanden-Eijnden, Comm. Pure Appl. Math. **61**, 1052 (2008).

[27] The origin of the term *caustic* follows from its use in geometric optics [see, for example, J. F. Nye, *Natural Focusing and Fine Structure of Light: Caustics and Wave Dislocations* (IOP Publishing, London, 1999)], and reflects the underlying mathematical similarity between light rays in optics and the optimal trajectories that arise as solutions to stochastic differential equations.

[28] Because the theory we have used up to this point was derived using the Itô calculus, we need to convert Eq. (19) to Itô form. In doing so, a diffusion-gradient drift term appears. For the magnetic dynamics studied, this extra drift term is $\hat{\mathbf{B}} \cdot \nabla_{-\mathbf{m}} \cdot \hat{\mathbf{B}}^T = -\frac{\alpha}{2\xi}\mathbf{m}$. Since, in computing the norm of the drift, we keep terms only of order α or higher, the only extra contribution to the drift norm is given by a term proportional to $|\mathbf{m} \cdot (\mathbf{m} \times \mathbf{h}_{\text{eff}})| = 0$.

[29] The usual formulation of the spin-torque term does not include a factor of α; it is not a dissipative term. We include it here because it is convenient to define the current in terms of α: $I \sim J/\alpha$, where J is the spin current pumped into the system per unit time. The reason for doing this is so the critical current I_C for switching [defined between Eqs. (25) and (26)] is independent of α: $I_C = J_C/\alpha = (2/\pi)\sqrt{D(D+1)}$.

[30] D. Pinna, A. D. Kent, and D. L. Stein, Phys. Rev. B **88**, 104405 (2013).

[31] D. Pinna, D. L. Stein, and A. D. Kent, Phys. Rev. B **90**, 174405 (2014).

[32] L. Ye, G. Wolf, D. Pinna, G. D. Chaves-O'Flynn, and A. D. Kent, J. Appl. Phys. **117**, 193902 (2015).